1

Introduction

T. Arai

1.1 The Discovery of X-Rays and Origin of X-Ray Fluorescence Analysis

The development of the modern theory of atomic structures was initiated based on the discovery of X-rays (1895). It was further triggered by the awareness of the existence of electrons in the atom, which was clarified by the line splitting observed when applying an external magnetic field (1896) and by the scattering of alpha particles at the atomic nucleus (1910). During the past few decades, X-ray physics has not only inspired and supported various research and development in the natural sciences, but has also had a beneficial impact on medical applications [1]. In today's civilized world, X-ray technology continues to play an important role in the advancement of material science, inspections in production processes, and diagnostics for medical treatment.

Cited below are two evolutional events in the history of X-ray science.

Watson and Crick proposed the DNA structure based on biological and structural chemistry including X-ray crystal structure analysis. Wilkins precisely studied the crystal structure using a rotating crystal method. The consolidation of their works led to the determination of the double helical structure of DNA, which has a three-dimensional structure of a screwed ladder and a regular arrangement of the four bases: adenine, thymine, guanine, and cytosine in the space between the two ladder poles [2].

The combination of the high X-ray transparency of the human body and its use for medical treatment brought about a notable advance in the use of X-rays for medical applications. Oldendorf planned to develop a relevant instrument in 1960. Then, Cormack presented his idea that included a mathematical treatment for three-dimensional imaging in 1963 and 1964. As Hounsfield used a radioactive source, a long time was required for taking a picture. Finally, he developed a computer-assisted tomogram using the consolidated technology of X-ray tube radiation, X-ray detectors, and computer calculations for the

preparation of three-dimensional pictures of X-ray intensity and indications for easy and precise diagnosis. Clinical data were presented in 1972 and 1973. Many instrumental improvements led to high-grade medical treatment that was founded on the present X-ray machine [3].

On November 8, 1895, Wilhelm Conrad Röntgen discovered X-rays in his laboratory at the physics institute of Julius-Maximilians University of Würzburg in Bavaria. He had studied cathode rays using an air-filled Hittorf-Crooks tube, which was shaded with a black paper. The tube wall was hit by electrons and emitted light. In his darkened room, he noticed a weak luminescence which radiated from a fluorescent screen located near the tube. He recognized "eine neue Art von Strahlen" (a new type of rays), which originated from the tube. After changing the experimental and surrounding conditions, he was able to observe the emission of weak rays of light on the fluorescent screen. He announced the new experimental results. It was immediately recognized that this discovery might be used to look into the structure of a living human body and the interior of constructed materials [4, 5].

After the announcement by Röntgen, two further important discoveries were made: radioactivity from uranium by Becquerel (1896) as well as radium and polonium by Marie and Pierre Curie (1898).

Using an aluminum filter method for the separation of X-rays and an ionization chamber for X-rays detection, Barkla studied the nature of X-rays relative to the atomic structure. Observing the secondary X-rays which were radiated from a target sample, he discovered the polarization of X-rays (1906), the gaps in atomic absorption (1909), and the distinction between continuous and characteristic X-rays, which consisted of several series of X-rays, named the K, L, M ... series (1911). The intensity and distribution of continuous X-rays were dependent on the number of electrons in an atom, and the characteristic X-rays were related to the electron energy configuration in the atom [6]. In succession to Barkla's works, the wave properties of X-rays were investigated by von Laue, who exhibited X-rays diffraction from a single crystal, which was composed of a three-dimensional structure with a regularly repeating pattern (1912). The experimental results showed the comparability of the wavelength of X-rays with the atomic distances and confirmed the wave properties of X-rays.

W. H. Bragg, who derived the famous Bragg's formula, was interested in von Laue's experiments. Using a Bragg spectrometer, the X-ray reflection patterns from single crystals of NaCl and KCl were observed to be the regular patterns of an isometric system showing differences in the X-ray intensity when comparing sodium and potassium. This was the starting point of crystal structure analysis with X-rays [7].

For the expansion of radiographic technology, the need for a heavy-duty X-ray tube emerged. After the tungsten filament (1908) and the tungsten incandescent lamp (1911) were invented, Coolidge developed a new type of tube setting, successfully solving the problem of low power and instabilities of

a gas-filled discharge tube. In this new tube, thermal electrons emitted from a hot filament hit the target, which was an emission source of X-rays (1913) [8].

Following the investigation of the properties of X-rays by Barkla, Moseley studied characteristic X-rays in an exchange of communications with W.L. and W.H. Bragg. He put target samples into a gas-filled discharge tube, which were then irradiated with electrons for the generation of characteristic x-rays. The narrow collimated characteristic X-rays hit the cleaved surface of a $K_4Fe(CN)_6 \cdot H_2O$ crystal and the third-order lines of Bragg reflection X-rays were obtained, which were shown in the famous photograph taken in 1913 [9]. Moseley elucidated the relationship between the characteristic X-rays and the measured elements, and communicated his experimental results to Bohr [10].

Siegbahn produced an X-ray spectrometer for a wider range of characteristic X-rays. He measured the wavelengths of characteristic X-rays precisely and classified them into $\alpha, \beta, \gamma \ldots$ according to the X-ray intensities in the respective series. X-ray spectroscopy was established with these works (1913–1923).

In the next advances, Hadding tried to analyze rare earth elements using the X-ray method. His work was supported by Siegbahn.

Due to the establishment of the structure of atoms, it became possible to predict the existence of elements that had yet to be discovered. This was based on the assumption that undiscovered elements belonging to the same family of elements in the periodic table have the same chemical features. In this respect, hafnium was isolated by von Hevesy and Coster (1923) [11] and rhenium by Noddack and Tacke with the support of Berg (1925).

During the initial stage of the use of X-ray spectroscopy for chemical analysis, the samples being analyzed were modified (or even destroyed) when electron excitation was applied, leading to changes in the X-ray intensities. Hadding, Glocker, and Frohnmayer pointed out the analytical problems of inter-element effects in quantitative analysis. When electron excitation was used, Coster and Nishina noticed sample evaporation because of the induced heat in the sample (1925), and Glocker and Schreiber found concentration changes in the constituent elements (1928). For the emission of characteristic X-rays in X-ray spectrochemical analysis, the X-ray excitation method was adopted as a non-destructive analysis method. Although the relative distance between the X-ray source and sample was reduced to increase the primary X-ray intensity, the resultant X-ray intensity was still insufficient to be measured [12]. On the positive side background X-rays became lower and, as a result for quantitative analysis, low intensity peaks could be measured easily.

For the measurement of X-ray intensities an ionization chamber or a photographic plate had been used. Perrin invented the ionization chamber in 1896, which was used in Barkla's works and adopted in Bragg spectrometers. In 1928, Geiger and Müller produced a new useful counter for the detection of γ-rays and X-rays, called the Geiger-Müller counter. Although analytical

principles and procedures had been studied in the academic field, the development of X-ray analytical instruments for general use had to wait until the end of the Second World War.

During the Second World War, the precise measurement of the cutting angle of quartz was required in mass production of oscillation plates. For this purpose, an X-ray apparatus was built by Parrish and Gordon based on a modified Bragg ionization chamber spectrometer (1945) [13]. Based on production experiences of the X-ray apparatus, Friedman introduced detectors for γ-rays and X-rays, as well as sensing head systems for various X-ray applications (1947) [14]. Then he started to develop a prototype X-ray spectrometer for the measurement of diffracted X-ray intensities and Bragg angles. Adopting a new Geiger-Müller counter and an electronic pulse counting unit (1947), a quartz plate which was located at the rotation center of a goniometer was replaced with a solidified powder sample (1945) [15].

When the iron-containing samples were measured using a Cu target X-ray tube, an abnormal increase in X-ray intensity was found, because the iron fluorescent X-rays radiating from a diffraction sample had strayed into the detector. As a result of the realization that fluorescent X-rays could be detected easily by this measuring system, a new X-ray fluorescence spectrometer was built. Analytical problems of measuring weak fluorescent X-ray intensities were encountered in the 1920s and the 1930s, which changed the requirements for the improvement of instrumentation. Friedman and Birks adopted a high power X-ray tube with a large window which gave rise to an increase in the effective solid angle, contributing to a short distance between the x-ray source in the x-ray tube and the sample to be analyzed. On the goniometer that is used in X-ray diffraction measurements, a bundle of narrow nickel pipes was used for collimation. Based on the need for a large reflecting surface, high reflecting power and relatively small lattice spacing, NaCl and fluorite crystals were chosen (1948) [16]. Figure 1.1 shows the X-ray fluorescence spectrometer developed by Friedman and Birks.

Expanding upon Friedman and Birks' work, Abbott was successful in building the first commercial X-ray fluorescence spectrometer in 1948 [17]. These works can be regarded as the beginning of modern X-ray spectrometry.

1.2 Historical Progress of Laboratory X-ray Fluorescence Spectrometers

In this section, the historical progress and important developments of the wavelength dispersive method in laboratory X-ray instruments are briefly reviewed.

In 1964, Birks, one of the pioneers of the X-ray fluorescence spectrometer, visited Japan and delivered a lecture "X-ray fluorescence: Present limitations and future trends." In his lecture, the analytical limits achievable in those days were reviewed covering elements from sodium to uranium, the detectability of

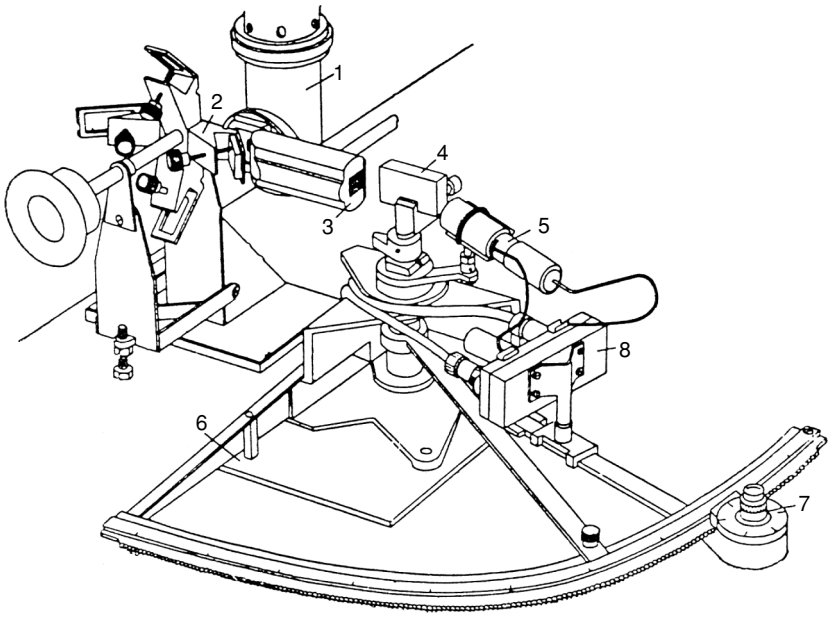

Fig. 1.1. The X-ray fluorescence spectrometer by Friedman and Birks [16].
1, X-ray tube; 2, specimen holder; 3, Soller collimator; 4, crystal; 5, Geiger counter; 6, base plate; 7, vernier for setting and reading the angular position of the crystal; 8, pre-amplifier

ppm order, the analytical precision of about 1%, and the possible analytical error caused by the matrix effects [18]. Concerning the anticipated further progress of the analytical method, he directed attention to the measurement of light and ultralight elements, sample preparation, improvement of excitation and detection of X-rays, utilization of computers for spectrometer control and analytical calculation as well as to the energy dispersive method appearing just then.

In 1976, Birks reviewed again the principles of X-ray fluorescence analysis and the progress of analyzing techniques including the instrumentation and the evaluation of the new methods. In this review, he emphasized the progress in the matrix correction method and the fundamental parameter method, which were led by the evaluation of the X-ray tube spectrum. In addition, some applications and future expectations were discussed [19].

In 1990, Gilfrich made a survey of X-ray fluorescence analysis. He directed attention to the new X-ray source, namely, the synchrotron radiation and to the introduction of synthetic mutilayers as analyzing crystals, to advanced X-ray technologies such as TXRF and EXAFS, semiconductor detectors for energy dispersive techniques, and to the significant progress of data handling with small computers [20].

Furthermore, in 1997, Gilfrich [21] gave a retrospect on the historical development of X-ray analysis during the past 100 years in commemoration of the discovery of X-ray by W.C. Roentgen.

Against the backdrop of such constructive remarks and the popularization of the X-ray fluorescence spectrometer, there have been many kinds of X-ray instruments developed for various measuring purposes, so that the instruments available today have gone ahead of the prediction by Birks in terms of type and number.

An X-ray analysis system configured with a X-ray diffractometer and an X-ray fluorescence spectrometer was introduced by Parrish [22]. As both equipments were provided with a high voltage power supply for an X-ray tube and shared a pulse counting system , it was widely utilized in laboratory applications. In addition, this spectrometer was equipped with a helium attachment for measuring soft X-rays.

Spielberg, Parrish, and Lowitzsch described the functional elements of nonfocusing optics and the geometrical condition for their harmonizing combinations [23]. They used a closer coupling of an X-ray tube for the sample and a large solid angle of primary X-rays for higher fluorescent intensity. Consequently, the inhomogeneity of fluorescent intensity distribution arising from the change of irradiating density of primary X-rays on the sample was brought forth. Their equipment was based on the Bragg spectrometer and had a parallel beam optics composed of a flat analyzing crystal and a double Soller collimator. Furthermore, the X-ray tube, the composed X-ray optics, and a sample container for primary X-ray irradiation were assembled in such a way as to embody convenience of use.

Arai pointed out that the total reflection from a metal sheet of a Soller collimator broadened a peak profile in its tails [24]. In addition, he studied the aberration of peak profiles caused by the vertical (the direction parallel to the goniometer rotation axis) divergence, reflection profiles from imperfect single crystals, and spectral overlapping [25].

Campbell and Spielberg, and Parrish and Lowitzsch studied a double Soller collimator on the basis of a flat crystal X-ray optics [23, 26].

Arai proposed as a practical solution that the horizontal divergence of a sub-Soller collimator should be two or three times larger than that of the main collimator, which was dependent on the grade of mosaic structure of analyzing single crystals.

For the analysis of the light elements, a helium and vacuum path spectrometer was offered by Miller and Zingaro for laboratory-use instruments [27].

An X-ray spectrometer for industrial applications, equipped with parallel beam optics and named Autrometer, was developed by Miller and Kiley in 1958. It was equipped with a step scanning goniometer, a tandem detector connecting a scintillation counter and a gas flow proportional counter, and adapted with a helium path for light element analysis. The spectrometer further incorporated the intensity ratio method designed to maintain the X-ray intensity stability upon referring to the standard sample intensity for quantitative determination [28, 29].

Equipments other than the scanning (and parallel-beam-optics) spectrometers, pursuing the basic features of rapid and high precision analysis for industrial applications, are the spectrometers equipped with multi-channel fixed goniometers.

Kemp developed the first combination model of scanning and fixed channel multi-element X-ray spectrometer based on the development and production of an optical emission spectrometer [30].

Furthermore, Jones, Paschen, Swain, and Andermann proceeded with the development of this advanced X-ray equipment, which adopted the focusing circle optical system with curved crystals, the detectors with the gas discrimination, and the direct capacitor accumulation of electric signals of the detector [31]. In order to obtain a higher intensity of measuring X-rays, focusing optics were adopted using Johann or Johansson curved crystals. In the case of the scanning goniometer, a curved single crystal moved in a straight line away from the entrance slit on the focusing circle, and then the detector slit on the focusing circle crawled along the four-leaf rose locus. The distance between the entrance slit and the curved crystal center was proportional to the wavelength of the measuring X-rays. The gas discrimination in the detector had a favorable effect on the intensity reduction of backgrounds and overlapping X-rays. The capacitor accumulation method was effective to measure a high counting rate of analyzing X-rays.

For light element analysis of cement samples, a helium path was adopted by Andermann, Jones, and Davidson [32], and then Andermann and Allen intensified the X-ray analysis of various materials related to cement industry. Additionally, a vacuum spectrometer was developed for light element analysis of cement and steel production applications by Dryer, Davidson, and Andermann [33]. In order to procure high intensity stability of the measuring X-rays and compensate the matrix effect, an X-ray monitoring method to detect scattered X-rays from the sample was introduced into the intensity measuring system by Andermann and Kemp [34]. However, the aforementioned capacitor accumulation and the monitoring method were changed to the absolute intensity measurement using pulse-counting circuits with a clock timer and the pulse selection method later.

Anzelmo and Buman presented a combined instrument which contained a scanning goniometer and several fixed goniometers in one spectrometer, in 1983 at the Pittsburgh Conference. This was a new concept of adaptable use in an analytical laboratory [35].

In 1995, Kansai, Toda, Kohno, Arai, and Wilson developed a fixed channel-multi-element spectrometer provided with 40 fixed goniometers by adopting logarithmic-spiral curved crystal monochromators. For high speed analysis, high counting rate X-ray intensity measurement of 10 to 50 million counts per second was carried out with a pure material by means of a combination of an X-ray beam attenuator and high speed electronic circuits with fast counting rate response. In the meanwhile, for the impurity analysis of various ores or high purity materials, two receiving slits located beside each other, one for

a fluorescent peak and the other for the background, were equipped in a goniometer for background correction calculation [36].

The core technology of an X-ray spectrometer consists of the excitation of fluorescent X-rays, the X-ray optics, and matrix correction calculations based on the fundamental parameter method. Described in this section are the remarkable progress and development in X-ray optics. Other features will be touched upon in the following section.

1.3 Measurement of Soft and Ultrasoft X-Rays

The purpose of conducting soft and ultrasoft X-ray measurements is to study the emission spectra influenced by chemical bonding or to make a quantitative determination of low atomic number elements. For the study of emission spectra, a high resolution spectrometer, and for quantitative determination, a high intensity one are required, respectively. The analytical problems in a quantitative determination of low atomic number elements originate from the inherent performance caused by the low excitation efficiency of soft X-rays and low reflectivity of spectroscopic device.

1.3.1 X-Ray Tubes for Soft and Ultrasoft X-Rays

In earlier days, most of the X-ray tube manufacturers supplied a side window tube with a thick beryllium window (about 1 mm thick) for spectrometer use. Inasmuch as these X-ray tubes are almost inefficient for X-ray measurement of light elements owing to the low excitation efficiency, new X-ray tubes with chromium and scandium target were developed on the basis of the side window structure by Kikkert and Hendry [37]. Characteristic K-radiation from this new tube passing through a relatively thin beryllium window can effectively excite the fluorescent X-rays of light elements.

Caldwell used a General Electric XRD 700 spectrometer equipped with a dual target (W, Cr) tube [38]. For heavy element measurement, the tungsten target, and for light element measurement like titanium and silicon in high alloy steel, the chromium target, were used, respectively. The analytical errors for titanium and silicon could be reduced. It demonstrated an improvement in the analytical accuracy of light elements by increasing the soft X-ray excitation efficiency.

Mahn of Machlett Laboratories Inc. developed an end window X-ray tube with a thin beryllium window and a rhodium target [39]. In order to minimize the secondary electron bombardment effect on the thin beryllium window, the target surface was charged with positive potential and the cathode filament was earth-grounded. The L series X-rays from the rhodium target are effective for excitation in soft and ultrasoft X-ray regions while the K series X-rays from the target are effective for heavy element analysis.

Gurvich compared various X-ray tubes and emphasized the advantage of the end window X-ray tube for light element analysis [40].

In scientific works by Henke, a specially designed demountable X-ray tube for soft and ultrasoft X-ray excitation was developed [41]. Using a very thin window or working without a window, an aluminum target for emission of Al-K lines or a copper target for Cu-L lines was adopted. The target was charged with positive potential and the filament was earth-grounded to protect the tube from window damage.

Indispensable features of dispersive devices are a large d-spacing according to the Bragg equation, high reflectivity due to the crystal structure, and low absorption. Single crystals having relatively large d-spacing as in EDDT, ADP, and KAP have been used at the beginning, and later on, PET and TlAP came into use for soft X-ray measurement.

In ultrasoft X-ray measurement, the role of dispersive devices has been classified into two categories: to the first category belong high resolution optics for profile studies based on single crystals, soap multilayered pseudo crystals, and grating dispersive analyzers, while the second category consists of high reflectivity devices for measurement of elemental concentration using total reflection mirrors, and later on, synthetic multilayer analyzers. X-ray analyzers and dispersing principles are shown in Fig. 1.2.

1.3.2 Scientific Research Work on Soft and Ultrasoft X-Rays

Holliday studied the fine structure of emission lines of O-Kα, C-Kα and B-Kα and of the L-band of titanium, vanadium, and manganese, upon which chemical bonding has direct effects, using electron bombardment excitation of X-ray emission lines, curved grating optics, and a gas flow proportional counter for X-ray detection [42]. C-Kα X-ray profiles of the F-C system were studied, to which belong graphite, Fe_3C, and mixtures of martensite and austenite.

Fischer and Baun investigated X-ray emission lines influenced by chemical bonding using electron bombardment excitation [43]. Studies of K-series of beryllium, boron, carbon, and nitrogen, of the L-band of sulfur, chlorine, and potassium, K-series of magnesium, aluminum, and silicon, and self-absorption effects were carried out by use of flat crystals of EDDT, ADP, and a soap pseudo crystal, and a gas flow proportional counter.

Henke observed narrow profiles with low background intensity owing to the lack of short wavelength X-ray components in the primary beam, using the previously mentioned X-ray tube, flat soap multilayer pseudo crystals which were developed by means of the Langmuir–Blodgett dipping method, and a gas flow proportional counter with an ultrathin window [44].

1.3.3 Synthetic Multilayer Analyzers

As reviewed by Barbee, the attempts to develop synthetic multilayer (SML) analyzers have a long history [45]. Today's SML analyzers had been introduced into practical use in 1975–1985. Spiller tried to produce SML analyzers using

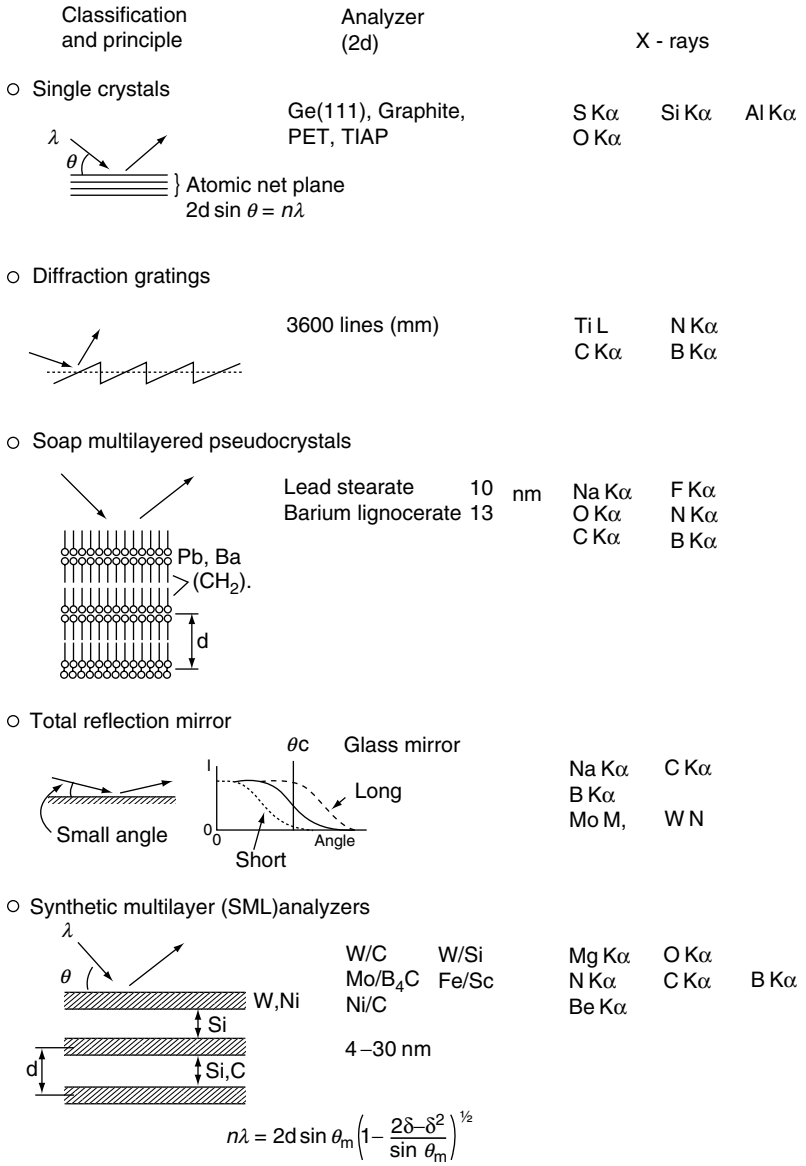

Fig. 1.2. Various X-ray analyzers for soft and ultrasoft X-rays and their principles

a thermal evaporation method controlled by a quartz crystal oscillator [46]. Barbee and Underwood exhibited the theory of X-ray reflection and observed reflection profiles of various X-rays including C-Kα X-rays using an SML analyzer [47].

Using the sputtering method, thin layers of reflecting and spacing films were arranged alternately on a substrate with smooth surface. Reflecting material selected from high reflectivity substances and spacing material having low absorption within the considered X-ray region were chosen. The total layer thickness equal to the sum of the thickness of reflecting and spacing layers is 2–20 nm and the total number of accumulated multilayers is 30–100 layers.

For soft X-ray measurement, Gilfrich, Nagel, Loter, and Barbee studied the feasibility of the development of SML analyzers by comparing a RAP crystal with a W/C SML upon observation of the peak profiles and reflecting intensity of the Al-Kα line [48].

Arai, Shoji, and Ryon carried out an ultrasoft X-ray measurement, using a standard laboratory spectrometer equipped with a rhodium target end window tube and a W/C analyzer [49]. The first detection of Be-Kα X-rays from beryllium–copper alloys was performed by Toda, Kohno, Araki, Arai, and Hamill [50]. The analytical precision at 1.75 wt% beryllium was 0.034 wt% and the accuracy in the concentration range of 0.2–2.0 wt% was 0.01 wt%.

Boron oxide in glasses in the concentration range of 2.5–19 wt% was analyzed with a precision of 0.4 wt% at the concentration of 10 wt% and an accuracy of 0.9 wt% under the condition that B-Kα lines were superimposed by the third order lines of O-Kα X-rays.

Boron in boron-contained stainless steel used for a radioactive material container was analyzed with a precision of 0.01wt% at the concentration of 0.76 wt% and an accuracy of 0.03 wt% in the range of 0.1–1.6 wt%.

Carbon concentrations in steel were measured with a precision of 0.015 wt% at 1 wt% and the accuracy was two or three times higher than the precision. It was necessary to correct for the overlapping interference of W-N, Mo-M and Fe-L lines and for the influence of absorption of silicon in matrix material. In the case of X-ray measurement of oxygen and nitrogen, the strong absorption by carbon in matrix constituents was discovered.

Anzelmo and Boyer investigated the analytical performance of SML analyzers using an end window tube with a rhodium target and showed the potential for ultrasoft X-ray measurements [51].

Huang, Fung, and White evaluated various SML analyzers for the measurement of B-Kα, C-Kα, N-Kα and O-Kα X-rays. They showed an increase in the reflective intensity corresponding to the increase of d-spacing [52].

The increase of the observed Bragg angle of SML analyzers due to refraction effects of long wavelength X-rays was pointed out by Martins and Urch [53].

Based on the work of Huang and his co-workers on thin film characterization using the fundamental parameter method [54], Arai accomplished the simultaneous determination of thickness and constituent elements in thin layered materials using soft and ultrasoft X-rays [55]. The analysis of PSG and BPSG layers, which are used as covering materials for semiconductor memory devices, was also carried out. The achieved analytical precision and

Table 1.1. Analytical precision and accuracy of PSG, BPSG, and SiO_2 films [55]

		Thickness (nm)	P_2O_5 (wt%)
PSG	Precision	3.6–3.8	0.07–0.09
	(range)	(700)	(14–22)
	Accuracy	6.4–15.5	0.15–0.4
	(range)	(1100–1500)	(2.2–25)

		Thickness (nm)	P_2O_5 (wt%)	B_2O_3 (wt%)
BPSG	Precision	1.6–2.8	0.02–0.06	0.06–0.14
	(range)	(530–1040)	(12–14)	(2–7)
	Accuracy	6.2–9.2	0.1–0.5	0.12–0.35
	(range)	(420–1080)	(0–27)	(0.02–13)

		Thickness (nm)
SiO_2	Precision	0.07
	(range)	(7.6)
	Accuracy	0.2
	(range)	(1.0–15)

accuracy of film thickness and concentration of constituent materials are given in Table 1.1. O-Kα X-rays were used for the sake of film thickness measurement of a thin-layered SiO_2 on a silicon wafer. It was demonstrated that very thin layers of SiO_2 can be measured.

White and Huang carried out thickness measurements of a carbon film in a double-layered structure of carbon and Co Cr alloy on a silicon wafer. The analytical precision of 2% for a 25 nm thick layer could be obtained using a W/C SML analyzer with 4 min of counting time [56].

Kobayashi and his co-workers studied analytical problems regarding the use of an SML analyzer and made the following observations [57].

Pure metals of aluminum or silicon emit the fluorescent X-rays of the Al-L or Si-L series. However, when oxide materials are irradiated, the fluorescent X-rays of the Al-L or Si-L series disappear because an outer electron of silicon or aluminum metal moves to oxygen. Covering a metallic surface of aluminum or silicon with a thin layered film of their oxide, their L lines emitted from the metallic substance penetrate the oxide layer and lead to a long tail of radiation at the short wavelength side. The latter interferes with the measuring X-rays increasing the background radiation.

If short wavelength X-rays emitted from an analyzed sample hit an SML analyzer, fluorescent X-rays generated from constituent elements of the SML stray into the X-ray detector and eventually contribute to the increase of the SML background radiation. Furthermore, some part of the fluorescent radiation interferes with reflecting net planes yielding Bragg reflection radiation.

Long wavelength X-rays emitted from an analyzed sample are reflected totally from the surface of an SML analyzer and as a result, an increase in background radiation can be seen occasionally.

When higher order reflections of short wavelength X-rays emitted from a sample interfere with the analyzing radiation, an SML analyzer modified by an appropriate choice of the thickness ratio of reflecting to spacing layers is used to suppress the higher order X-ray reflections.

1.3.4 Total Reflection Mirrors

In order to obtain a higher intensity of measuring X-rays, electron bombardment excitation was adopted. For soft X-ray measurement, Franks and Braybrook used X-ray optics consisting of the combination of a collimator, a total reflection mirror, and a windowless photomultiplier, as shown in Fig. 1.3 [58].

Herglotz improved the measuring system for soft X-ray measurement, shown in Fig. 1.3 [59]. Using electron bombardment excitation, the measuring system was made up of a curved surface paraffin mirror, receiving slit, and a windowless photomultiplier. Later on, an X-ray excitation method was developed for routine applications [60].

Arai sought for practical solutions to measure ultrasoft X-rays and demonstrated that the combination of a rhodium target end window tube with a thin beryllium window and a total reflection mirror along with a selected filter could be applied for the detection of B-Kα, C-Kα, N-Kα and O-Kα lines using a standard X-ray fluorescence spectrometer. The quantitative determination of boron oxide in boron glasses, carbon in steel, nitrogen in various chemical compound substances, and oxygen in coal were carried out [60]. Boron oxide in glasses in the range of 1 to 20 wt% could be analyzed with a precision of 0.2 wt% at lower concentration and 0.42 wt% at 19 wt%; the analytical accuracy was 0.65 wt% corrected with K_2O and PbO. Carbon in carbon steel, cast iron, and stainless steel were measured. The analytical error composed of X-ray intensity precision and grinding effect error on the sample surface was about 0.01% in carbon and stainless steel and 0.01 wt% at the concentration of 3.82 wt% in cast iron. The accuracy was 0.01–0.02 wt% in carbon and stainless steel and 0.05 wt% in the range of 2–4 wt% in cast iron. Overlapping influences of molybdenum, niobium, tungsten, and tantalum and an absorption influence of matrix effect of silicon were found [60]. Oxygen measurement in coal or iron ores and nitrogen measurement in various materials were carried out and matrix effects were studied for the improvement of accuracy.

For industrial application, Sugimoto, Akiyoshi, and Kondou studied the determination of carbon in pig iron and obtained analytical results for carbon in the range of 3.5–4.7 wt% with a reproducibility of 0.05 wt% and an accuracy of 0.083 wt% using a Rigaku multi-fixed channel spectrometer provided with a total reflection mirror for the detection of C-Kα X-rays [61].

Comparing an SML analyzer with a total reflection mirror along with an optimized filter in the X-ray separating system, it can be said that the SML analyzer offers a wider applicable method because of high resolution profiles and low background X-ray intensity.

Franks and Braybrook (1959) [58]

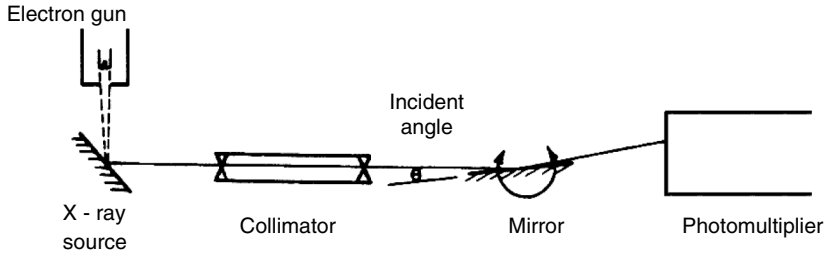

Herglotz (1967) [59]

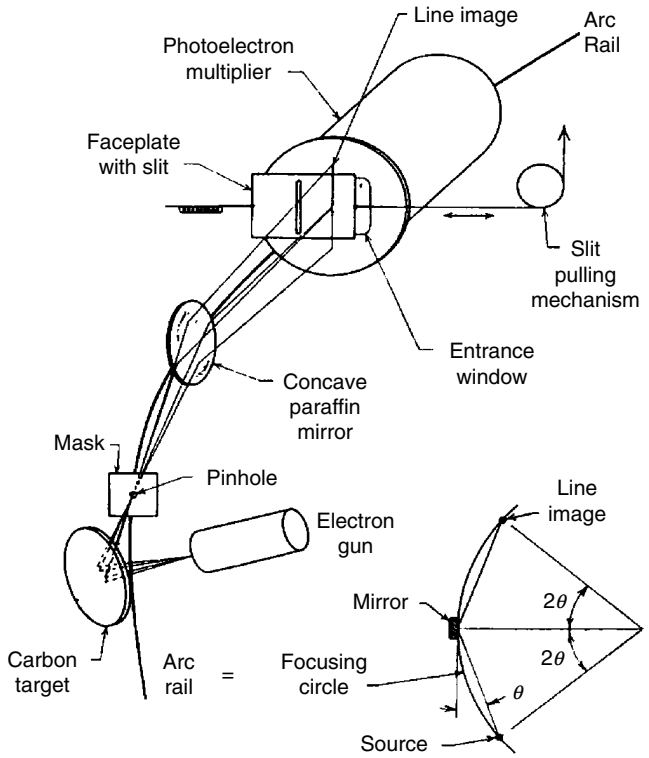

Fig. 1.3. Historical succession of the development of X-ray fluorescence spectrometers for light element analysis

Additionally, to conclude this section, it can be stated that at present the quantitative potentiality of soft and ultrasoft X-ray fluorescence analysis depends decisively on the efficiency of the end window X-ray tube with a thin beryllium window and a rhodium target as well as on the high reflectivity of the SML analyzer.

Henke (1964) [41][44]

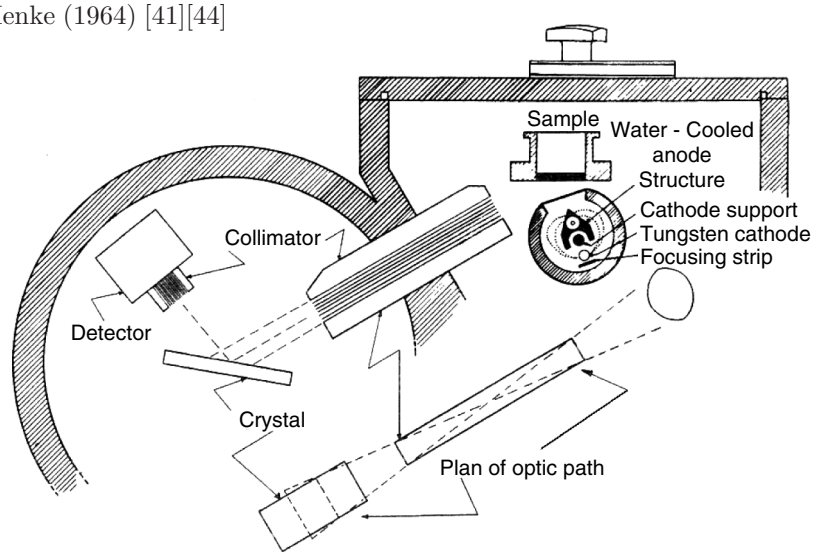

Rigaku (1982) [60]

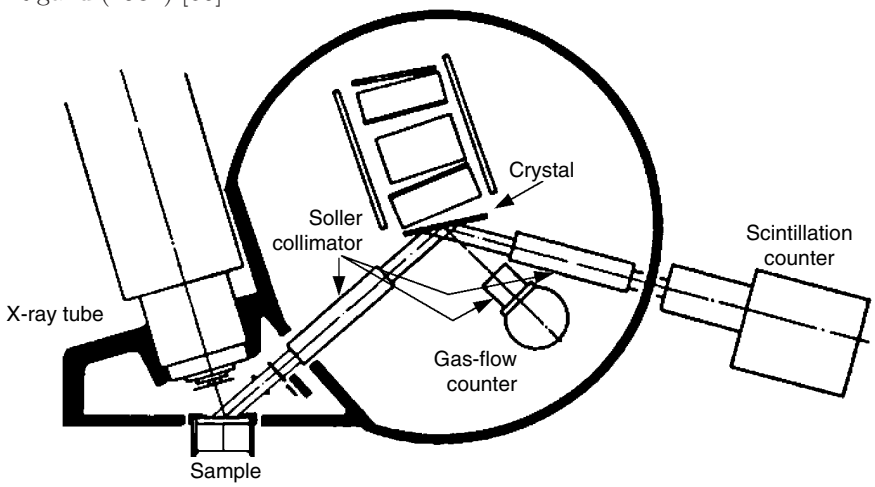

Fig. 1.3. *Continued*

1.4 Analytical Precision and Accuracy in X-Ray Fluorescence Analysis

When an analytical sample is irradiated with X-rays emitted from an X-ray tube or radioactive source, fluorescent X-rays are generated in the sample and can be measured for quantitative analysis of its constituent elements. X-ray fluorescence analysis is rapid, precise, and nondestructive.

From the standpoint of X-ray intensity measurement, Zemany made a summary of precision and accuracy [62]. In this section, the X-ray matrix effect, which is the most basic and the largest component in analytical accuracy, is concisely discussed by comparing X-ray accuracy with X-ray precision (see subchapter 5.9 for further details).

X-ray intensity, or the accumulated count of measured X-ray photons per unit time, is always accompanied by a statistical fluctuation which conforms to the Gaussian distribution with a standard deviation equal to the square root of the total counts. The precision of an X-ray measurement can, therefore, be predicted by the measured intensity. For example, an accumulated intensity of 1,000,000 counted X-ray photons has a standard deviation of 0.1%, and for 100,000,000 counts the standard deviation is 0.01%.

When an X-ray beam propagates through a sample, its intensity is modified by matrix element effects, concurring with the generation of characteristic X-rays, absorption of the emitted X-rays along their paths, and the enhancement effect due to secondary excitation. Studies of these modification processes and related X-ray physical phenomena lead to the derivation of mathematical correction formulae. The development of these X-ray correction methods dominates the analytical performance of the X-ray fluorescence method.

1.4.1 Correction of Matrix Element Effects

The advances in X-ray fluorescence instruments and applications have led to the need for the development of practical and effective mathematical correction formulae. A number of correction methods have been developed (see for example, Lachance and Traill [63], Rassberry and Heinrich [64], etc.). Beattie and Brissey derived a basic correction formula for the relationship between the intensity of characteristic X-rays and the weight fraction of constituent elements, which was the product of a term containing the intensity of measured analytical X-rays and a correction factor containing the concentrations of the constituent elements [65].

A classification of the correction equations published in the literature is carried out from the standpoint of mathematical simplicity and shown in the following:

1. The correction term attributed to constituent elements consists of a constant plus the sum of the products of an X-ray intensity and a correction coefficient, or the sum of the products of a weight fraction and a correction coefficient.
2. The correction coefficients may or may not include the term with the analytic element.
3. The correction coefficients are mostly treated as constants, and this assumption is efficient in the case of small concentration changes of constituent elements.

4. In order to develop wider applicable correction equations and improve the elimination of analytical errors, terms with variable correction coefficients are used in the correction formulae, which are affected with the third or the fourth constituent elements.
5. Least-squares methods have been used for the determination of correction coefficients and correction equations by using experimental data from a large number of standard samples. However, after the development of the fundamental parameter method, calculated intensities have been used for the derivation of correction coefficients and equations as well as for the verification of experimentally determined coefficients and equations. Since there exist many correction methods for quantitative analysis, it is necessary for practical applications to know about the characteristics of matrix correction equations to select the proper fitting algorithm for the analyzed sample.

Rousseau reviewed the concept of the influence of coefficients in matrix correction method from the standpoint of theoretical and experimental approaches and he admonished the essence of a fundamental parameter method [66].

The development of the fundamental parameter method has been carried out by a number of X-ray scientists. At first, Sherman [67] studied the generation of characteristic X-rays theoretically. Shiraiwa and Fujino [68] proceeded with this method even more accurately and verified it experimentally. For the spectral distribution of a primary X-ray source, they combined Kulenkampff's formula [69] of continuous X-rays with their own measured intensity ratios of continuous X-rays and tungsten L series X-rays from a side window X-ray tube. Criss and Birks [70] developed the method further by measuring the primary X-ray intensity distributions from side window X-ray tubes and using mini-computer systems to control X-ray fluorescence spectrometers [71].

To improve the performance of an X-ray spectrometer, a high-power end window X-ray tube with a thin beryllium window was developed by Machlett Laboratories, Inc. [39]. A remarkable improvement in the analytical performances for light elements was achieved by a close coupling of the X-ray source with the sample and a high transmittance window. In order to accomplish a reliable fundamental parameter method, the primary X-ray distributions from end window X-ray tubes were measured by Arai, Shoji, and Omote. It was found that the output of the X-ray spectral distribution in the long wavelength region was increased [72].

Figure 1.4 shows the comparison between measured and calculated intensities of various steels and alloy metals. At low concentrations background intensity corrections should be applied and at the higher intensity ranges the measured intensity requires a counting loss correction. Samples used in Fig. 1.4 are shown in Table 1.2.

Using calculated X-ray intensities, matrix correction coefficients and correction equations have been inspected, and methods using variable correction

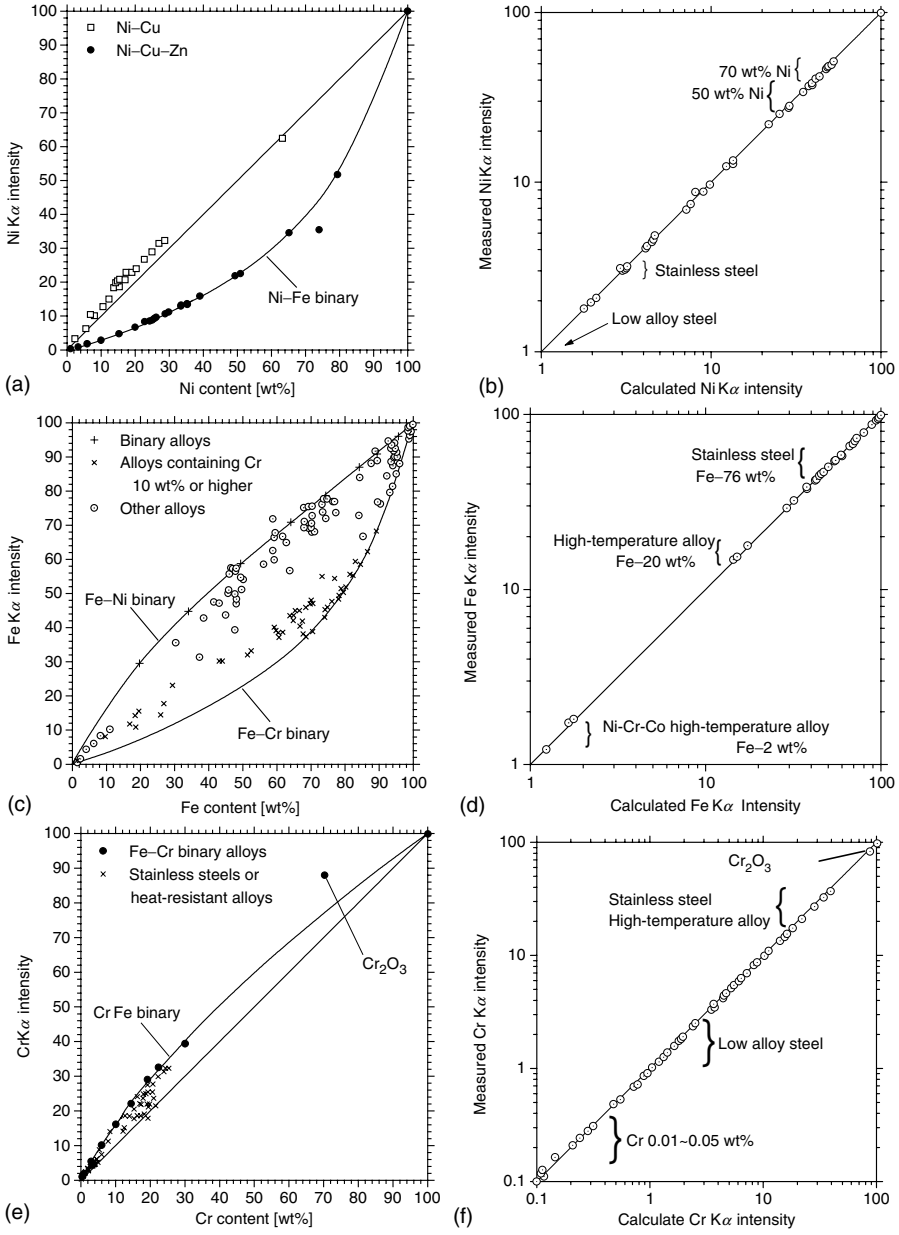

Fig. 1.4. (**a**) Relationship between nickel concentration and Ni-Kα intensities, (**b**) Relationship between iron concentration and Fe-Kα intensities, (**c**) Relationship between chromium concentration and Cr-Kα intensities, (**d**) Comparison between calculated and measured Fe-Kα intensities, (**e**) Comparison between calculated and measured Fe-Kα intensities, (**f**) Comparison between calculated and measured Cr-Kα intensities

Table 1.2. Measured samples in Fig. 1.4

Low alloy steel	Heat-resistant steel	Tool steel	Magnetic alloy
Stainless steel	High-speed steel	Binary alloy	German silver
High-temperature alloy	Magnetic steel		

coefficients have been derived for high accuracy analysis and wider applicable correction equations. Rousseau [73] showed comparative figures of measured and calculated X-ray intensities and applied them to the correction equations developed by Claisse and Quintin [74] and Criss and Birks [70].

Furthermore, Rigaku Industrial Corporation.. tried to compare the measured intensity with calculated intensities based on its own developed fundamental parameter method. Using the primary X-ray distribution from the end window X-ray tube, precisely matching calibration curves were obtained. Using these curves, direct quantitative analysis was then carried out by iterative computer algorithms without the need of matrix correction equations. The analytical results for high alloy analysis are shown in the following section.

1.4.2 Quantitative Analysis of Heat-Resistant and High-Temperature Alloys

Gould [75] summarized metal analysis with X-ray spectrochemical analysis. In this section, matrix correction and some segregation influencing analytical accuracy are discussed in detail.

Abbott who was the first developer of a commercial X-ray fluorescence spectrometer, presented a strip chart record of high alloy steel (16-25-6) shown in Fig. 1.5 [17]. Compared to modern equipment, his spectrometer gave much weaker intensities and poorer spectral resolutions due to adoption of a Geiger counter and a NaCl analyzing crystal. Figure 1.6 is a spectrum of NBS 1155 high alloy steel measured with a modern instrument, which equips a scintillation counter and a LiF analyzing crystal. Since the fluorescent intensities and spectral resolution are sufficiently high for practical applications, the difference between these two pictures exhibits the historical progress of 50-years development.

As pointed out by Abbott, the X-ray method is well suited for analyzing heat-resistant and high temperature alloys which consist of nickel, cobalt, iron, and chromium as major constituents, and low concentrations of various other elements. Because the concentrations of the constituent elements influence the metallurgical properties of high temperature and heat-resistant alloys, high precision is required in quantitative determination. In order to review the analytical accuracy of numerous reports, a comparison parameter is introduced, defined as the root mean square between chemical analysis and non-corrected or corrected X-ray values (abbreviated as RMS-difference). Studies of RMS-differences were performed and are shown in Table 1.3.

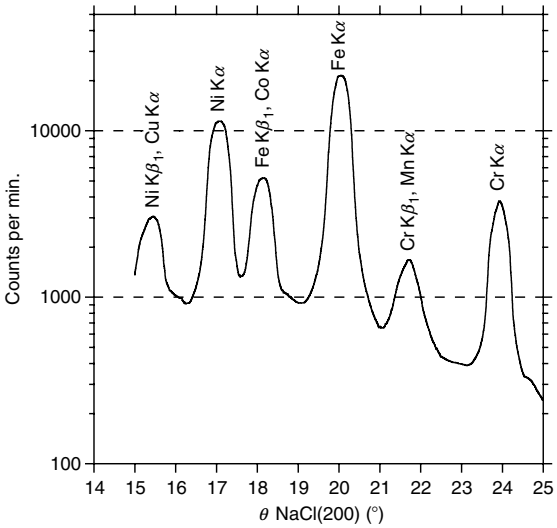

Fig. 1.5. Spectrum of 16-25-6 alloy taken by Abbott [17]

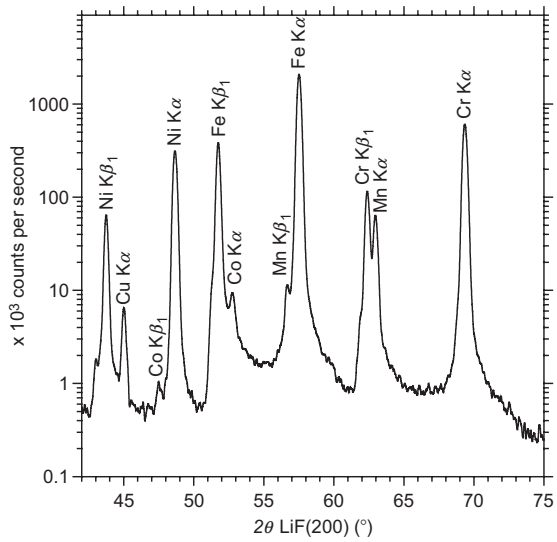

Fig. 1.6. Sepctrum of NBS 1155 taken by using Rigaku ZSX 100e

Rickenbach [76] showed the precision and accuracy of nickel and chromium analysis. The measured precision of nickel and chromium in an A286 metal was shown as the composite error within a day and extending to several days. The mean value of the nickel error was 0.03 wt% at the concentration

Table 1.3. RMS-difference in heat resistance steel and high temperature alloy analysis. The upper value is the RMS-difference and the lower is the concentration range of the element in each cell. "Sum difference" means the RMS-differences between wt% sums of chemical and X-ray analysis of the analyzing elements. All values are in wt%

#	Measurements	Analyzed elements							
		Al	Si	P	S	Ti	V	Cr	Mn
1	Rickenbach (1963)							0.11 14 ∼15	
2	Lucas-Tooth and Pyne (1964)							0.07 7 ∼ 26	0.032 4 ∼ 10
3	Gillieson, Reed, Milliken and Young (1964)					0.034 0.0 ∼ 3.6		0.36 0.3 ∼33	0.029 0.0 ∼ 1.6
4	Lachance and Traill (1966)					0.10 0.0 ∼ 3.6		0.97 4 ∼ 33	0.11 0.0 ∼ 2
5a	Caldwell (1976)		0.014 0.1 ∼ 1.1			0.016 0.1 ∼ 0.5		0.19 0.05 ∼ 25	0.045 0.2 ∼ 1.9
5b	*ditto*		0.013 0.1 ∼ 1.1			0.016 0.1 ∼ 0.4		0.098 0.05 ∼ 25	0.023 0.2 ∼ 1.9
6	Ito, Sato and Narita (1983)	0.056 0.9 ∼ 10	0.024 0.2 ∼ 2.1	0.002 0.∼0.022		0.052 1.0 ∼ 11	0.021 0.2 ∼ 2.2	0.14 5 ∼ 28	0.023 0.5 ∼ 3.5
7a	Griffiths and Webster (1986)	0.026 0.4 ∼ 5.6	0.039 0.0 ∼ 0.6			0.026 0.0 ∼ 3.8		0.28 8 ∼ 25	0.013 0.0 ∼ 0.6
7b	*ditto*	0.025 0.0 ∼ 5.6	0.039 0.0 ∼ 0.6			0.027 0.0 ∼ 3.8		0.078 8.8 ∼ 25	0.012 0.0 ∼ 0.6
8	Itoh, Sato, Ide and Okochi(1986)	0.047 0.8 ∼ 5.8				0.13 0.2 ∼ 4		0.29 8 ∼ 22	0.006 0.0∼0.07
9	Rigaku (2000)	0.024 0.0 ∼ 1.4	0.023 0.07∼1.0	0.0009 0.0∼0.02	0.0009 0.0∼0.02	0.026 0.0 ∼ 3.1		0.10 15 ∼ 22	0.010 0.08∼1.4

Table 1.3. *Continued*

#	Analyzed elements									Sum
	Fe	Co	Ni	Cu	Zr	Nb	Mo	Ta	W	difference
1			0.19 25 ∼ 27							
2										
3	0.38 0.1 ∼ 96	0.28 0.0 ∼ 64	0.45 0.0 ∼ 78		0.014 0.0 ∼ 0.5	0.046 0.0 ∼ 2.0	0.05 0.0 ∼ 17	0.014 0.0 ∼ 0.5	0.09 0.0 ∼ 18	0.51
4	1.1 0.1 ∼ 28	3.7 0.0 ∼ 64	1.9 0.7 ∼ 78			0.22 0.0 ∼ 4.7	0.29 0.0 ∼ 25		0.55 0.0 ∼ 18	3.1
5a	0.47 14 ∼ 90		0.40 0.3 ∼ 81	0.031 0.1 ∼ 0.6		0.014 0.2 ∼ 0.7	0.10 0.0 ∼ 4.4			0.20
5b	0.34 14 ∼ 90		0.06 0.3 ∼ 81	0.031 0.0 ∼ 0.6		0.014 0.2 ∼ 0.7	0.013 0.01∼4.4			0.22
6	0.16 4.6 ∼ 56	0.073 2.0 ∼ 30	0.23 31 ∼ 96	0.032 0.2 ∼ 6.4	0.009 0.1 ∼ 0.8	0.066 0.8 ∼ 9.4	0.088 1 ∼ 28	0.047 0.2 ∼ 10	0.069 1 ∼ 12	
7a	0.039 0.1 ∼ 3.5	0.11 0.5 ∼ 20	(48 ∼75)	0.055 0.0 ∼ 0.3	0.057 0.0 ∼ 0.3	0.015 0.0 ∼ 1.0	0.009 0.0 ∼ 11	0.015 1.3 ∼ 2.6	0.058 0.0 ∼ 10	0.38
7b	0.044 0.0 ∼ 3.5	0.12 0.5 ∼ 20	0.17 47 ∼ 76	0.015 0.0 ∼ 0.3	0.010 0.0 ∼ 0.3	0.009 0.0 ∼ 1.0	0.009 0.0 ∼ 11	0.016 0.0 ∼ 2.6	0.031 0.0 ∼ 10	0.39
8	0.074 0.0 ∼ 7.2	0.38 0.2 ∼ 13				0.025 0.1 ∼ 2.0	0.053 0.1 ∼ 9.		0.030 0.03 ∼ 10	
9	0.19 1.4 ∼ 67	0.035 0.0 ∼ 21	0.29 9.4 ∼ 74	0.005 0.0 ∼ 0.1		0.020 0.0 ∼ 5.4	0.014 0.0 ∼ 5.4	0.007 0.0 ∼ 0.4	0.015 0.0 ∼ 2.4	0.48

Table 1.3. *Continued*

#	X-ray instrument	Tube target	Matrix correction	Number of Samples	Reference
1	GE XRD-5 (Sequential)	-	Simple calibration method. No matrix correction	22	[76]
2	Solartron automatic vacuum spectrometer XZ1030	-	Lucas-Tooth and Pyne method. Intensity correction	60 (Cr) 3 (Mn)	[77]
3	Norelco 100kV	W	Lachance - Traill method Fixed a correction	25	[78]
4	Philips 100kV	W		80	[81]
5a	GE XRD-700 (Sequential)	Cr (for Si and Ti) W (heavy elements)	Lachance - Traill method Fixed a correction	80	[80]
5b	*ditto*	*ditto*	Lachance - Traill method Variable a correction	*ditto*	*ibid.*
6	Rigaku Simultix 4B (Fixed channels)	Rh	JIS correction	80	[82]
7a	Philips 1410 (Sequential)	Cr	Lachance - Traill method with small modification (Standard)	14	[83]
7b	*ditto*	*ditto*	Lachance - Traill method with small modification ("60:20:20" correction)	*ditto*	*ibid.*
8	Philips 1400 (Sequential)	Rh	de Jongh's theoretical correction coefficients	7	[85]
9	RigakuZSX100e (Sequential)	Rh	Confrontation method between measured and calculated intensity based on FP	12	-

of 26.2 wt% and for chromium it was 0.023 wt% at 14.5 wt%. They are one-fifth of the RMS-differences in Table 1.3. It was noted that no matrix corrections were required for specimens with only small concentration variations.

Lucas-Tooth and Pyne discussed a formula where the correction factor was a constant plus the sum of products of the individual X-ray intensities of the constituent elements with correction coefficients. RMS-differences of 0.07 wt% in chromium and 0.032 wt% in manganese were reported [77].

A third report sponsored by the ASTM committee in 1964 was presented by Gillieson, Reed, Milliken, and Young [78]. Simultaneously, a report about spectrochemical analysis of high temperature alloys by spark excitation was presented. Referring to the matrix correction methods by Lucas-Tooth and Price [79] and Lucas-Tooth and Pyne, they applied a correction on the basis of X-ray intensities of the constituent elements. The measured intensities of aluminum and silicon constituents should be added in order to improve the matrix correction, thereby increasing the accuracy.

Lachance and Traill studied simple matrix correction equations that were one plus the sum of products of the weight fraction of constituent elements and correction coefficients [63]. Based on the analysis of high nickel alloys that were selected from the application report, RMS-differences were calculated and are shown in Table 1.3.

On the basis of the Lachance–Traill equations, Caldwell derived two kinds of correction equations [38]. The first one was a fixed correction coefficient equation and the second one was a variable correction coefficient equation for wider concentration applications, on which the third or fourth constituent elements exerted reform. RMS-differences of major constituents in variable correction coefficient calculations improved those of the fixed correction coefficient method.

Ito, Sato, and Narita [82] studied the JIS correction equations that consisted of the product of a factor containing a quadratic polynomial of the intensity of the measured X-rays, and a matrix correction factor which was authorized by the JIS Committee. The coefficients of the intensity part were determined by least-squares algorithms from binary alloys with known chemical composition or from mathematical models, and the second factor was one plus the sum of products of the weight fractions of the constituent elements and correction coefficients, in which the terms containing the base component and the analyzing elements were excluded. In practical applications for nickel base alloys the correction coefficients of light and heavy elements from iron-based alloys were used; for the analysis of the major constituent elements, chromium, iron, and cobalt in nickel base alloys, the correction coefficients were determined experimentally.

Griffiths and Webster discussed the derivation of matrix correction equations in detail. They adopted the modified Lachance–Traill equation [83]. The calibration constants of the X-ray intensity terms were determined by regression analysis and the correction factors were calculated with the ALPHAS program which was theoretically derived by de Jongh [84]. The two kinds of RMS-differences of authenticated sample analysis are shown in Table 1.3. The

values in the upper line are the calculated results based on normal matrix correction in the ALPHAS program, and the second values in the lower line are derived with the use of correction coefficients calculated under the condition of a fixed 60:20:20 constituent sample.

Itoh, Sato, Ide, and Okochi studied the analysis of high alloys using the theoretically calculated correction coefficients of the ALPHAS program. They also compared the ALPHAS program and the JIS correction method and clarified that there were no differences between them. The results of analytical accuracy were two or more times higher than those of X-ray analytical precision [85].

Rigaku Industrial Corporation analyzed high nickel alloys of NBS and specially prepared samples. For the matrix correction, they adopted their own fundamental parameter method and prepared calibration curves, which were used for the determination of the constituent elements. The RMS-differences in these studies were fairly small.

1.4.3 Segregation Influencing Analytical Accuracy

The influence of inhomogeneity phenomena on analytical accuracy is one of the most important factors. The internal soundness of an ingot which was studied by Marburg [86] conferred that the inhomogeneity induced in the cooling process from molten metals intimated strong effects to analytical problems to be solved.

Stoops and McKee studied the reduction of analytical accuracy for titanium concentrations owing to segregation of nickel base alloys of M252 (19 wt% chromium, 10 wt% cobalt, 10 wt% molybdenum, 2.5 wt% titanium, 3 wt% iron, 1 wt% aluminum, 0.15 wt % carbon, and 0.35 wt% silicon). As a major portion of the titanium could be found in the grain boundaries of carbide or carbon-nitride particles, the differences between regular chemical and X-ray analysis values indicated a wider distribution, which was 5–10% of the amount of titanium present. When chemical analysis was carried out using samples scooped up from the X-ray analytical surface, X-ray values were nearly equal to that of chemical analysis, i.e., 0.5–1% of the amount of titanium present [87].

It is well known that in rapidly cooled steel, a low concentration of manganese and impurity sulfur are dispersed and that a high analytical accuracy in manganese and sulfur determination can be found. In sufficiently annealed steel, small particles of manganese sulfide are precipitated in the grain boundaries of steel grains and large deviations of Mn-Kα and S-Kα X-rays are found [88].

Free cutting metals that are among the most widely used industrial materials are typical examples for exhibiting segregation phenomena in metals. Small metal particles like lead in steels and copper alloys influence machine processing of high-speed cutting.

Iwasaki and Hiyoshi studied lead segregation in bronze alloys. Microscopic observations of the surface pictures of a cast bronze showed a mixture of ground metal of copper and lead precipitated particles, and the recast pictures showed the surface with scattering of small lead particles. Comparing surfaces of recast and cast samples, Cu-Kα X-rays from cast sample surface exhibited higher intensities and Pb-Lα X-rays showed lower intensities. In recast sample surfaces, Cu-Kα X-rays showed lower intensities and Pb-Lα X-rays higher intensities because of absorption of Cu-Kα X-rays and the exciting of bare surfaces of many small particles of lead on analyzing surface [89].

In the analysis of lead free cutting steels (Pb content: 0.1–0.3 wt%), small particles of lead metal (1–15 µm) are scattered in steel. Arai reported that simple repeatability of Pb-Lα X-rays was 0.003 wt% and RMS-difference of lead was 0.018 wt% [90].

The characteristics of segregation or inhomogeneity have been recognized as one of natural phenomena or as discoveries through experimental works. If some studies or works have attained success after long or hard work, possibilities of more success or discovery will be increased on the basis of research work and their process.

1.5 Concluding Remarks

Elemental analysis of materials is absolute or relative. Gravimetric analysis is a typical example of the former, while X-ray fluorescence and optical emission methods represent the latter. In the case of a relative analysis, standard samples are required, which are attached to reliable or authenticated analytical values supported by absolute analysis. The values guaranteed by absolute analysis are the mean values of volume analysis, while X-ray analytical values represent surface analysis with an information depth of 5–50 µm. In order to reduce the analytical uncertainty, which orginates from the differences between volume and surface analysis, homogeneous samples samples should be used. For the sake of reducing the effect of inhomogeneity on the sample surface, large analyzed surfaces of 3–10 cm^2 are recomended.

Since the analytical accuracy is defined by a combination of errors of chemical analysis, uncertainty in the measured X-ray intensity, and uncorrected matrix effects by the constituent elements,the observed accuracy can be reduced by effective matrix corrections adapted for X-ray analysis, and elimination of other systematic errors may be activated.

References

1. Segrè E, From X-rays to quarks: Modern physicists and their discoveries. W.H. Freeman & Co., New York (1980)
2. The Nobel Prize in Physiology or Medicine 1962 to Crick FHC, Watson JD, Wilkins MHF, for their discoveries concerning the molecular structure of nucleic acids and its significance for information transfer in living material

3. The Nobel Prize in Physiology or Medicine 1979 to Cormack AM and Hounsfield GN, for the development of computer assisted tomography. Cormack AM, Representation of a function by its line integrals, with some radiological applications. J Appl Phys **34**, 2722–2727 (1963)
4. Glasser O, Wilhelm Conrad Röntgen and the early history of the Röntgen rays. Norman Publishing, San Francisco (1993)
5. Mould RF, A century of X-rays and radioactivity in medicine: with emphasis on photographic records of the early years. Institute of Physics Publishing, Bristol and Philadelphia (1993)
6. Barkla CG, Polarisation in secondary Röntgen radiation. Proc R Soc Sect **A 77**, 247–255 (1906)
   Barkla CG, Sadler CA, The absorption of Röntgen rays. Philos Mag **17**, 739–760 (1909)
   Barkla CG, The spectra of the fluorescent Röntgen radiations. Philos Mag **22**, 396–412 (1911)
7. Bragg WL, The crystalline state volume I: A general survey. Bell & Heyman, London (1949)
8. Coolidge WD, A powerful Röntgen ray tube with a pure electron discharge. Phys Rev **2**, 409–430 (1913)
9. Jaffe B, Moseley and the numbering of the elements. Doubleday & Co., Garden city, New York (1971)
10. Rozental S, Niels Bohr: His life and work as seen by his friends and colleagues. Elsevier, New York (1985)
    Moore RE, Niels Bohr: The man, his science, and the world they changed. Knopf/Random House, New York (1966)
11. von Hevesy G, Chemical analysis by X-rays and its applications. McGraw-Hill, New York (1932)
12. Glocker R, Materialprüfung mit Röntgenstrahlen unter besonderer Berücksichtigung der Röntgenmetallkunde. Springer Verlag, Berlin (1936)
13. Parrish W, Gordon SG, Precise angular control of quartz-cutting with X-rays. Am Mineral **30**, 326–346 (1945)
14. Friedman H, Applications of electronic methods to the measurement of X-ray and gamma ray intensities. Ind Radiography **Summer**, 9–20 (1947)
15. Friedman H, Geiger counter spectrometer for industrial research. Electronics, 132–137 (1945)
16. Friedman H, Birks LS, A Geiger counter spectrometer for X-ray fluorescence analysis. Rev Scientific Instrum **19**, 323–330 (1948)
17. Abbott JL, X-ray fluorescence analysis. The Iron Age, 58–62 (1948); Abbott JL, X-ray fluorescence analysis. The Iron Age, 121–124 (1948)
18. Birks LS, X-ray fluorescence: Present limitations and future trends. X-ray Anal, Japan, **2**, 5–13 (1965) [in Japanese]
19. Birks LS, Current capabilities and future goals in X-ray spectroscopy. Pure Appl Chem **48**, 45–52 (1976)
20. Gilfrich JV, New horizons in X-ray fluorescence analysis. X-ray Spectrom **19**, 45–51 (1990)
21. Gilfrich JV, 100 years of progress in X-ray analysis. **39**, 29–39 (1997)
22. Parrish W, X-ray spectrochemical analysis. Philips Technical Rev **17**, 269–286 (1956)
23. Spielberg N, Parrish W, Lowitzsch K, Geometry of the non-focusing X-ray fluorescence spectrograph. Spectrochim Acta **13**, 564–583 (1959)

24. Arai T, The profile of the parallel optical system having a Soller slit in X-ray fluorescence spectrograph. X-ray Anal, Japan **2**, 139–153 (1965) [in Japanese]
25. Arai T, Studies of 2θ values and peak profiles in non-focusing X-ray fluorescent spectrometer. Adv X-ray Chem Anal, Japan **19**, 293–305 (1988) [in Japanese]
26. Campbell WJ, Leon M, Thatcher J, Flat crystal X-ray optics. Adv X-ray Anal **1**, 193–206 (1958)
27. Miller DC, Zingaro PW, The universal vacuum spectrograph and comparative data on the intensities observed in an air, helium, and vacuum path. Adv X-ray Anal **3**, 49–56 (1960)
28. Miller DC, Results obtained with the modified Norelco Autrometer. Adv X-ray Anal **1**, 283–295 (1958)
29. Kiley WR, A universal detector for the X-ray spectrograph. Adv X-ray Anal **2**, 293–301 (1959)
30. Kemp JW, Instrumentation for rapid spectrochemical analysis–Optical and X-ray emission monochromators and polychromators. Anal Chem **28**, 1838–1843 (1956)
31. Jones JL, Paschen KW, Swain HH, Andermann G, Components for X-ray polychromators. Adv X-ray Anal **1**, 471–482 (1958)
32. Andermann G, Jones JL, Davidson E, The evaluation of the PXQ for the analysis of cements and related materials. Adv X-ray Anal **2**, 215–227 (1959)
Andermann G, Allen JD, The evaluation and improvement of X-ray emission analysis of raw-mix and finished cements. Adv X-ray Anal **4**, 414–432 (1961)
33. Dryer HT, Davidson E, Andermann G, Vacuum X-ray instrumentation and its application to mill-products control. Adv X-ray Anal **5**, 477–485 (1962)
34. Andermann G, Kemp JW, Scattered X-rays as internal standards in X-ray emission spectroscopy. Anal Chem **30**, 1306–1309 (1958)
35. Anzelmo JA, Buman AI, Evaluation criteria for wavelength dispersive XRF instrumentation. Am Lab, 65–73 (1988)
36. Kansai K, Toda K, Kohno H, Arai T, Wilson R, Accurate measurement of trace elements using an innovative fixed goniometer for a simultaneous spectrometer. Adv X-ray Anal **38**, 691–698 (1995)
37. Kikkert J, Hendry G, Comparison of experimental and theoretical intensities for a new X-ray tube for light element analysis. Adv X-ray Anal **27**, 423–426 (1984)
38. Caldwell VE, A practical method for the accurate analysis of high alloy steels by X-ray emission. X-ray Spectrom **5**, 31–35 (1976)
39. Mahn GR, The OEG-75G—A new high power tube for X-ray fluorescent analysis. Cathode Press **22**, 41–46 (1965)
40. Gurvich YM, Comparison of various X-ray tube types for XRF analysis. Adv X-ray Anal **28**, 113–118 (1985)
Gurvich YM, An advanced end-window. XRF spectrometer for analysis of light elements. Am Lab, 103–111 (1984)
41. Henke BL, X-ray fluorescence analysis for sodium, fluorine, oxygen, nitrogen, carbon, and boron. Adv X-ray Anal **7**, 460–488 (1964)
Henke BL, Tester MA, Techniques of low energy X-ray spectroscopy (0.1 to 2 keV region). Adv X-ray Anal **18**, 76–106 (1975)
Henke BL, Techniques of low energy X-ray and electron physics. 50 to 1000 ev region. Norelco Reporter **14**, 75–83, 98 (1967)
42. Holliday JE, The use of soft X-ray fine structure in bonding determination and light element analysis. Norelco Reporter **16**, 84–91, 116 (1967)

43. Fischer DW, Baun WL, The influences of chemical combination and sample self absorption on some long wavelength X-ray emission spectra. Norelco Reporter **14**, 92–98 (1967)
44. Henke BL, Measurement in the 10 to 100 angstrom X-ray region. Adv X-ray Anal **4**, 244–279 (1961)
Henke BL, Microanalysis with ultrasoft x-radiations. Adv X-ray Anal **5**, 285–305 (1962)
Henke BL, Application of multilayer analyzers to 15–150 angstrom fluorescence spectroscopy for chemical and valence band analysis. Adv X-ray Anal **9**, 430–440 (1966)
Henke BL, Lent RE, Some recent work in low energy X-ray and electron analysis. Adv X-ray Anal **12**, 480–495 (1969)
45. Barbee TW, Sputtered layered synthetic microstructure (LSM) dispersion elements. AIP Conf Proc **75**, 131–145 (1981)
46. Spiller E, Evaporated multilayer dispersion elements for soft X-rays. AIP Conf Proc **75**, 124–130 (1981)
47. Underwood JH, Barbee TW, Synthetic multilayers as Bragg diffractors for X-rays and extreme ultraviolet: Calculations of performance. AIP Conf Proc **75**, 170–178 (1981)
48. Gilfrich JV, Nagel DJ, Loter NG, Barbee TW, X-ray characteristics and applications of layered synthetic microstructures. Adv X-ray Anal **25**, 355–364 (1982)
Gilfrich JV, Nagel DJ, Barbee TW, Layered synthetic microstructures as dispersing devices in X-ray spectrometers. Appl Spectrosc **36**, 58–61 (1982)
Gilfrich JV, Multilayered structures as dispersing devices in X-ray spectrometry. Analytica Chim Acta **188**, 51–57 (1986)
49. Arai T, Shoji T, Ryon RW, Wavelength dispersing devices for soft and ultrasoft X-ray spectrometers. Adv X-ray Anal **28**, 137–144 (1985)
50. Toda K, Kohno H, Arai T, Araki Y, Hamill G, Sensitivity improvement and stabilization for ultra light element analysis by X-ray spectrometry. Adv X-ray Anal **37**, 629–637 (1994)
51. Anzelmo JA, Boyer BW, The analysis of carbon and other light elements using layered synthetic microstructures. Adv X-ray Anal **30**, 193–200 (1987)
52. Huang TC, Fung A, White RL, Recent measurements of long wavelength X-rays using synthetic multilayers. X-ray Spectrom **18**, 53–56 (1989)
53. Martins E, Urch DS, Problems in use of multilayers for soft X-ray spectroscopy and analysis: A comparison of theoretically and experimentally determined refraction effects. Adv X-ray Anal **35**, 1069–1078 (1992)
54. Huang TC, Thin film characterization by X-ray fluorescence. X-ray Spectrom **20**, 29–33 (1991)
55. Arai T, An X-ray fluorescent spectrometer for the measurement of thin layered materials on silicon wafers. Adv X-ray Anal **30**, 315–323 (1987)
56. White RL, Huang TC, Determination of ultra-thin carbon coating thickness by X-ray fluorescence technique. Adv X-ray Anal **32**, 331–339 (1989)
57. Kobayashi H, Toda K, Kohno H, Arai T, Wilson R, The study of some peculiar phenomena in ultra-soft X-ray measurements using synthetic multilayer crystals. Adv X-ray Anal **38**, 307–312 (1995)

Kobayashi H, Toda K, Kohno H, The study of some peculiar phenomena in ultra-soft X-ray measurements using synthetic multilayer crystals. Adv X-ray Chem Anal, Japan **26**, 45–58 (1995) [in Japanese]
58. Franks A, Braybrook RF, Analysis of the lighter elements by total reflexion of their characteristic X-ray wavelengths. Br J Appl Phys **10**, 190–191 (1959)
59. Herglotz HK, Wavelength identification of ultrasoft X-rays by the critical angle of total reflection. J Appl Phys **38**, 4565–4568 (1967);
Davies RD, Herglotz HK, A total reflection X-ray spectrograph for fluorescence analysis of light elements. Adv X-ray Anal **12**, 496–505 (1969)
60. Arai T, Soft and ultrasoft X-ray fluorescent spectrometer using total reflection monochromator. Japanese J Appl Phys **21**, 1347–1358 (1982)
Arai T, Sohmura T, Tamenori H, Determination of boron oxide in glass by X-ray fluorescence analysis. Adv X-ray Anal **26**, 423–430 (1983)
Arai T, Ohara S, Determination of oxygen and nitrogen in various materials by X-ray fluorescence spectrometry. Adv X-ray Anal **27**, 547–556 (1984)
Arai T, Measurement of soft and ultrasoft X-rays with total reflection monochromator. Adv X-ray Anal **30**, 213–223 (1987)
61. Sugimoto K, Akiyoshi T, Kondou T, XRF determination of carbon in pig iron. Bunseki Kagaku **37**, 589–594 (1988) [in Japanese]
62. Zemany PD, X-ray spectrometry Chapter 4. Precision and Accuracy. Marcel Dekker, New York, 69–110 (1978)
63. Lachance GR, Traill RJ, A practical solution to the matrix problem in X-ray analysis. Part 1: Method. Can Spectrosc **11**, 43–48 (1966)
64. Rassberry SD, Heinrich KFJ, Calibration for interelement effects in X-ray fluorescence analysis. Anal Chem **46**, 81–89 (1974)
65. Beattie HJ, Brissey RM, Calibration method for X-ray fluorescence spectrometry. Anal Chem **26**, 980–983 (1954)
66. Rousseau RM, Why the fundamental algorithm is so fundamental. Adv X-ray Anal **37**, 639–646 (1994)
67. Sherman J, The theoretical derivation of fluorescent X-ray intensities from mixtures. Spectrochim Acta **7**, 283–306 (1955)
68. Shiraiwa T, Fujino N, Theoretical calculation of fluorescent X-ray intensities in fluorescent X-ray spectrochemical analysis. Japanese J Appl Phys **5**, 54–67 (1966)
69. Kulenkampff H, Annalen der Physik **69**, 548 (1922)
70. Criss JW, Birks LS, Calculation methods for fluorescent X-ray spectrometry empirical coefficients vs. fundamental parameters. Anal Chem **40**, 1080–1086 (1968)
Criss JW, Birks LS, Gilfrich JV, Versatile X-ray analysis program combining fundamental parameters and empirical coefficients. Anal Chem **50**, 33–37 (1978)
71. Gilfrich JV, Birks LS, Spectral distribution of X-ray tubes for quantitative X-ray fluorescence analysis. Anal Chem **40**, 1077–1080 (1968)
Gilfrich JV, Burkhalter PG, Whitlock RR, Warden ES, Birks LS, Spectral distribution of a thin window rhodium target X-ray spectrographic tube. Anal Chem **43**, 934–936 (1971)
Brown DB, Gilfrich JV, Measurement and Calculation of Absolute X-Ray Intensities. J Appl Phys **71**, 4044–4046 (1971)
Brown DB, Gilfrich JV, Peckerar MC, Measurement and calculation of absolute intensities of X-ray spectra. J Appl Phys **46**, 4537–4540 (1975)

72. Arai T, T. Shoji, K. Omote, Measurement of the spectral distribution emitted from X-ray spectrographic tubes. Adv X-ray Anal **29**, 413–422 (1985)
73. Rousseau RM, Fundamental algorithm between concentration and intensity in XRF analysis. 1-Theory. X-ray Spectrom **13**, 115–120 (1984)
Rousseau RM, Fundamental algorithm between concentration and intensity in XRF analysis. 2-Practical application. X-ray Spectrom **13**, 121–125 (1984)
74. Claisse F, Quintin M, Generalization of the Lachance-Traill method for the correction of the matrix effect in X-ray fluorescence analysis. Can Spectrosc **12**, 129–146 (1967)
75. Gould RW, X-ray spectrometry Chapter 11. Metals and alloys. Marcel Dekker, New York, 277–295 (1978)
76. Rickenbach JR, Some aspects of nondestructive X-ray spectrochemical analysis of alloys. Adv X-ray Anal **6**, 352–360 (1962)
77. Lucas-Tooth J, Pyne C, The accurate determination of major constituents by X-ray fluorescent analysis in the presence of large interelement effects. Adv X-ray Anal **7**, 523–541 (1963)
78. Gillieson, AH, Reed DJ, Milliken KS, Young MJ, X-ray spectrochemical analysis of high-temperature alloys, ASTM Special Technical Publication No.376, 3–22 (1964)
79. Lucas-Tooth HJ, Price BJ, A mathematical method for the investigation of inter-element effects in X-ray fluorescence analysis. Metallurgia **64**, 149–152 (1961)
80. Lachance GR, Traill RJ, A practical solution to the matrix problem in X-ray analysis. Part 2: Application to a multielement alloy system. Can Spectrosc **11**, 63–71 (1966)
81. Caldwell VE, A practical method for the accurate analysis of high alloy steels by X-ray emission. X-ray Spectrom **5**, 31–35 (1976)
82. Ito M, Sato S, Narita M, X-ray fluorescence analysis of nickel base alloys. Tetsu-to-Hagan **69**, 169–176 (1983) [in Japanese]
Ito M, Sato S, Narita M, Comparison of Japanese industrial standard and a-correction method for X-ray fluorescence analysis of steel. X-ray Spectrom **10**, 103–105 (1981)
83. Griffiths JM, Webster HWM, X-ray analysis of nickel-base alloys with theoretically derived inter-element correction coefficients. X-ray Spectrom **15**, 61–72 (1986)
84. de Jongh WK, X-ray fluorescence analysis applying theoretical matrix corrections. Stainless steel. X-ray Spectrom **2**, 151–158 (1973)
85. Itoh S, Sato K, Ide K, Okochi H, X-ray fluorescence analysis of nickel-based heat-resisting alloys by matrix correction using theoretical alpha coefficients. Bunseki Kagaku **35**, 33–37 (1986) [in Japanese]
86. Marburg E, Accelerated solidification in ingots: Its influence on ingot soundness. J Metals, 157–172 (1953)
87. Stoops RF, McKee KH, Sampling errors in the X-ray fluorescent determination of titanium in a high temperature alloy. Anal Chem **33**, 589–592 (1961)
88. Bain EC, Functions of the alloying elements in steel, U S Steel Corporations, Pittsburgh PA, USA (1945)
89. Iwasaki K, Hiyoshi K, XRF analysis of bronze castings after recasting. Bunseki Kagaku **37**, 152–156 (1988) [in Japanese]
90. Arai T, Quantitative determination of lead in lead-free cutting steels. The Rigaku Denki J **3**, 207–208 (1961) [in Japanese]

http://www.springer.com/978-3-540-28603-5

Handbook of Practical X-Ray Fluorescence Analysis

Beckhoff, B.; Kanngießer, B.; Langhoff, N.; Wedell, R.;
Wolff, H. (Eds.)

2006, XXIV, 878 p., Hardcover
ISBN: 978-3-540-28603-5